ENGINEERING TRANSACTIONS • *Engng. Trans.* • **43**, 4, 627–635, 1995
Polish Academy of Sciences • Institute of Fundamental Technological Research

TRANSVERSE DEFLECTION OF A COLD-WORKED METAL PLATE CLAMPED AROUND ITS EDGE

R. L. BISH (MELBOURNE)

New principles are applied in an investigation of the general problem of a sheet of cold-rolled metal, clamped around its rim and displaced transversely. For the particular case of a circular cold-worked metal sheet clamped at its edge and displaced transversely at its centre by a flat-ended circular punch, it is predicted that the deflection will vary in proportion to the logarithm of radial distance from the punch axis, and that circles engraved on the sheet, concentric with the punch, will neither expand nor contract during deformation, while the punching load will remain proportional to the punch displacement and inversely proportional to the logarithm of the ratio of the clamp and punch diameters.

NOTATION

σ_{ij} stress tensor,
h yield function,
ε_{ij} strain tensor,
λ a multiplier,
k shear yield stress,
Y uniaxial tensile yield stress,
ω rotation rate,
w transverse deflection,
w_0 punch displacement,
σ_1, σ_2 principal stresses in the sheet,
ϕ_1, ϕ_2 rotations of elements about the respective σ_1- and σ_2-axes,
$\mathbf{b}$ unit vector parallel to the projection of the σ_1-axis on the horizontal (or initial) plane,
T initial sheet thickness,
C closed contour in the horizontal plane,
F force acting on material within C,
$\mathbf{n}$ unit vector normal to and drawn outwards from the region contained within C,
ds element of length along C,
dS element of area in C,
a punch radius,
b clamp radius,
r radial distance from punch axis.

1. Introduction

Well known theories of work-hardening [1] and plastic anisotropy [2] treat these two phenomena as distinct and, moreover assume initial isotropy. As such, of course, they can only be expected to exhibit restricted ranges of validity. Moreover, these theories impose taxing demands upon the experimentalist [3], who must measure the coefficients in them.

On the other hand, a new approach is possible in the case of metals that have already been cold-worked so as to exhibit a texture. In this new and simple theory [4], the crystal-grains of the solid rotate so as to align their crystallographic slip-planes parallel to the principal shear surfaces. This is how the texture develops but also the rotation rate vector (vorticity in hydro- or aero-mechanics) must also remain spatially continuous. For if this were not the case and two adjacent grains were to rotate at markedly different rates, than their slip-planes could not remain parallel to the local principal shear surfaces, which are required by equilibrium to remain smooth and continuous. We shall develop this idea directly.

In addition, a second principle follows from the above fact, that fully textured metals should obey Tresca's yield criterion, for each principal shear surface in a plastically deforming cold-worked solid is enveloped by crystallographic slip-surfaces, each of which is enclosed within a grain boundary. These slip-system must, collectively, offer a characteristic resistance to extended slip over the principal shear surface on which the resolved shear stress is the greatest.

2. Mathematical principles

2.1. Rotation rate

The domain D_1, shown in Fig. 1 within a closed contour C, is divided into a mesh of small domains d, each of which is enclosed by a contour c (we may view this mesh as the crystal-grain boundary network). Let $\mathbf{r}$ be the position vector of a point on c, measured from some fixed origin, O. Then by Stoke's theorem [5], if $\boldsymbol{\omega}$ denotes the rotation-rate vector,

$$\int_d \operatorname{curl} \boldsymbol{\omega} \cdot d\mathbf{S} = \int_c \boldsymbol{\omega} \cdot d\mathbf{r}, \tag{2.1}$$

where $d\mathbf{S}$ is an element of vector area on D_1. Since $\boldsymbol{\omega}$ is continuous so that contributions to $\boldsymbol{\omega} \cdot d\mathbf{r}$ from adjacent mesh elements are equal and opposite,

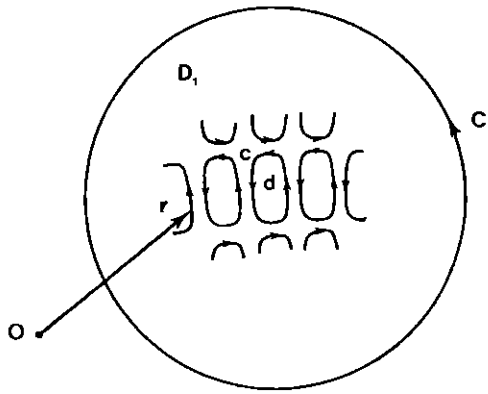

FIG. 1. Surface D_1 spanning a closed contour C.

and therefore cancel one another on summing, we obtain, on adding all the equations (2.1) for the mesh within C,

$$\int_{D_1} \operatorname{curl} \boldsymbol{\omega} \cdot d\mathbf{S} = \int_C \boldsymbol{\omega} \cdot d\mathbf{r}. \tag{2.2}$$

We may now repeat this operation for a second surface D_2 also spanning C and coinciding with D_1 over some region within C. Then by subtraction we obtain

$$\int_{D_1 D_2} \operatorname{curl} \boldsymbol{\omega} \cdot d\mathbf{S} = 0,$$

where the normal is drawn outwards from the closed surface $D_1 D_2$. Since $D_1 D_2$ is arbitrary it follows that

$$\operatorname{curl} \boldsymbol{\omega} = 0, \tag{2.3}$$

which, we have proved, is the necessary condition for the continuity of $\boldsymbol{\omega}$.

2.2. The yield condition

In Fig. 2a is shown a yield locus associated with Tresca's yield condition; which, as already pointed out, should be applicable to cold-worked metals. The six sides of the associated yield surface, in σ_{ij}-space, if σ_1, σ_2 and σ_3 are the principal stresses, are described by

$$\begin{aligned} \sigma_1 - \sigma_2 &= 2k, & \sigma_1 > \sigma_2 > \sigma_3, \\ \sigma_2 - \sigma_1 &= 2k, & \sigma_2 > \sigma_3 > \sigma_1, \\ \sigma_2 - \sigma_3 &= 2k, & \sigma_2 > \sigma_1 > \sigma_3, \end{aligned} \tag{2.4}$$

(2.4) [cont.]

$$\sigma_3 - \sigma_2 = 2k, \qquad \sigma_3 > \sigma_1 > \sigma_2,$$
$$\sigma_3 - \sigma_1 = 2k, \qquad \sigma_3 > \sigma_2 > \sigma_1,$$
$$\sigma_1 - \sigma_3 = 2k, \qquad \sigma_1 > \sigma_2 > \sigma_3,$$

where k denotes the shear yield stress of the solid. On the other hand,

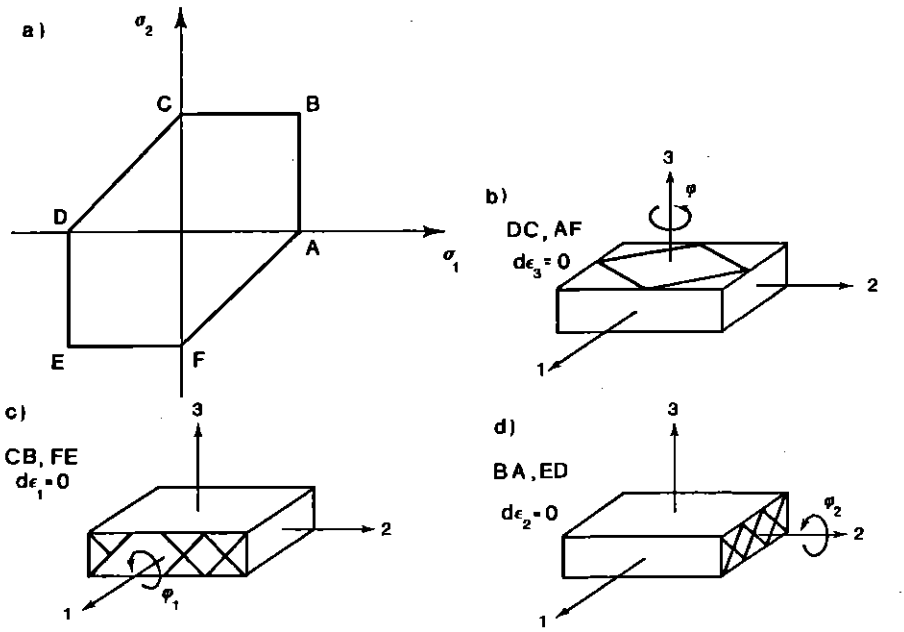

FIG. 2. Modes of deformation associated with the sides of the Tresca yield locus. In (b) the slip-lines remain inextensible, while in cases (c) and (d), one family of principal stress lines parallel to the plate remains inextensible.

writing

$$h(\sigma_1, \sigma_2, \sigma_3) = 0$$

for the yield surface, and $d\varepsilon_{ij}$ for the incremental strain tensor, PRAGER'S flow rule [6] requires that

$$d\varepsilon_{ij} = \frac{\partial h}{\partial \sigma_{ij}} d\lambda, \tag{2.5}$$

where λ is a multiplier. Substituting from (2.4) into (2.5) we obtain, in the case of a sheet, with n denoting the sheet normal and assuming σ_1 and σ_2 to lie within the sheet,

$$d\varepsilon_n = 0 \quad \text{for} \quad \sigma_1 - \sigma_2 = \pm 2k,$$
$$d\varepsilon_1 = 0 \quad \text{for} \quad \sigma_2 = \pm 2k,$$
$$d\varepsilon_2 = 0 \quad \text{for} \quad \sigma_1 = \pm 2k.$$

These equations remain true over the free surface of the sheet ($\sigma_n = 0$) and the modes of deformation described by the above equations are illustrated in Fig. 2; wherein the heavy lines in Figs. 2b, 2c and 2d indicate the traces of active slip surfaces. The rotations about the sheet normal and σ_1 and σ_2 axes are, respectively, ϕ, ϕ_1 and ϕ_2. It may be shown that (2.3) is equivalent (if we assume incompressibility) to the fact that the strain-rate tensor remains solenoidal. This fact was utilised in the earlier paper [4] to investigate the mode shown in Fig. 2b, to derive the properties of the Hencky-Prandtl net. In the cases shown in Figs. 2c and 2d, there is no Hencky-Prandtl net. The plate becomes curved, however, and so the interest shifts from the net angle to the plate deflection. For this reason we proceed directly from (2.3) in investigating those modes shown in Figs. 2c and 2d.

3. Transverse deflection of a clamped sheet

Figure 3 shows a section of a clamped and transversely deflected metal sheet. Let the σ_1- and σ_2 lines have projections in the initial plane of the

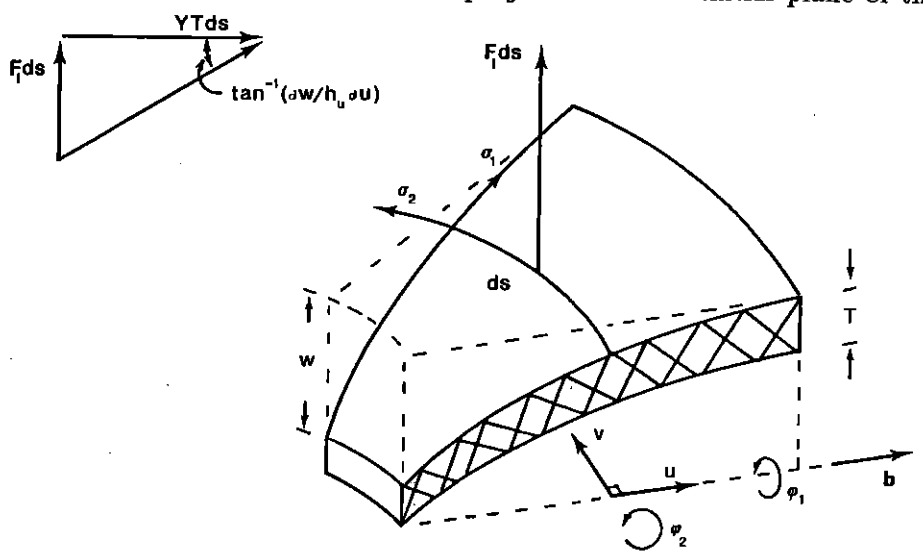

FIG. 3. Equilibrium of line forces.

sheet along which the respective coordinates are u and v, and the associated respective scale factors are h_u and h_v. Then if w is the transverse deflection, by the usual formula for the rotation-rate (or vorticity),

$$\phi_1 = \frac{1}{2}\frac{\partial w}{h_v \partial v}, \qquad \phi_2 = -\frac{1}{2}\frac{\partial w}{h_u \partial u}, \tag{3.1}$$

where the time-independent form is chosen because the boundaries are fixed. We also may re-express (2.3) in the time-independent form,

$$\frac{\partial}{\partial u}(h_v\phi_2) - \frac{\partial}{\partial v}(h_u\phi_1) = 0,$$

and substituting from (3.1) and using the formula [5]

$$h_u h_v \nabla^2 = \frac{\partial}{\partial u}\left(\frac{h_v}{h_u}\frac{\partial}{\partial u}\right) + \frac{\partial}{\partial v}\left(\frac{h_u}{h_v}\frac{\partial}{\partial v}\right),$$

we obtain

$$\nabla^2 w = 0. \tag{3.2}$$

4. Forces

Figure 3, in which σ_1 has been set equal to the uniaxial yield stress, $Y = 2k$, and T is the initial plate thickness, serves to show us how to calculate the vertical force on any line-element in the plate, if this line is parallel to the initial plane of the plate. In fact, if ds is the length of the element then the force F per unit length of the σ_2-lines is $YT\mathbf{b}\cdot\operatorname{grad} w$. On any closed contour C in the initial plane of the plate, the total (transverse) force is therefore given by

$$F = \int YT\mathbf{n}\cdot\operatorname{grad} w\, ds, \tag{4.1}$$

where $\mathbf{n}$ is the outward unit vector normal to C. If C encloses the punch then F equals the punching force. If C does not enclose the punch and lies outside its perimeter, then F vanishes. For if A is the area enclosed by C in the initial plane,

$$\int_C \mathbf{n}\cdot\operatorname{grad} w\, ds = \int_A \nabla^2 w\, dS,$$

by Gauss' divergence theorem, and this integral vanishes, by (3.2). Therefore the total force on the region within C also vanishes, as required by equilibrium.

Thus we see that the solution represented by zero extension along the σ_2-lines and equations (3.2) and (4.1) satisfies all of the requirements for a metal sheet that has been cold-worked so that it deforms by slip between elastic elements, the slip surfaces remaining parallel to the principal shear stress surfaces. The lines on which the sheet is clamped or displaced remain parallel to its initial plane and are not extended or reduced in length; these are lines of σ_2 (Fig. 3 and Fig. 2d).

5. An example

Applying the above theory to a circular disc, clamped at its edge and displaced by a flat-ended solid cylinder concentric with the clamp (Fig. 4), we first note that the σ_2-lines are now circles concentric with the punch. They remain circular and neither expand nor contract as the punch continues to be displaced, and so *the circles marked on the sheet surface concentric with the punch and clamp will neither expand nor contract* as the sheet is deflected. This result, of course, assumes sticking friction over the area of contact between the punch and sheet. From (3.2), moreover, if a denotes the punch radius and b the clamp radius, and if the shoulder of the punch is sharp,

$$w = \frac{w_0 \ln (r/b)}{\ln (a/b)}, \tag{5.1}$$

where r denotes radial distance from the axis, and w_0 is the punch displacement (Fig. 4). Thus we see that *the transverse deflection remains proportional to the logarithm of radial distance from the punch axis.*

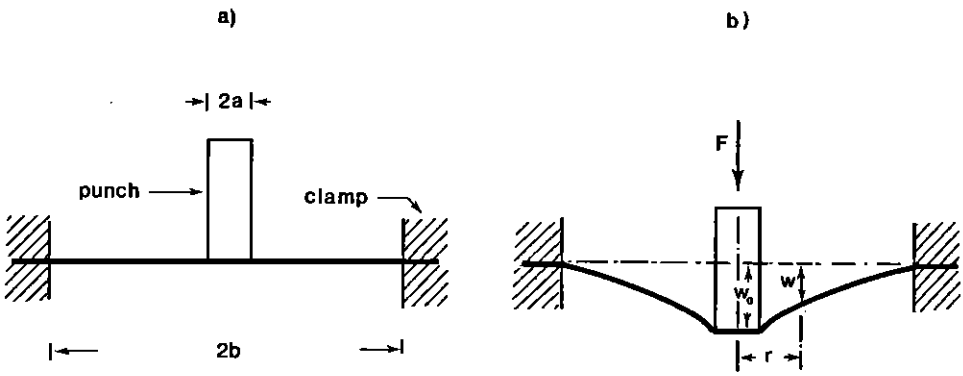

FIG. 4. Punching of a sheet clamped on a circle and deflected transversely by a concentric circular punch having sharp corners; a) before, b) after punching.

Finally from (4.1), using (5.1), we obtain for the punching force, assuming a mean value for Y,

$$F = \frac{2\pi T Y w_0}{\ln (a/b)}, \tag{5.2}$$

and this formula shows us that *the load-displacement relation is linear with a slope that remains inversely proportional to the logarithm of the ratio of the clamp and punch diameters.*

We should expect these conclusions to remain valid in cases where the sheet is made of *rolled copper or brass, or even rolled iron or strain-aged*

mild-steel. But we would not expect any of these assertions to apply in the case of, say, a fully annealed copper sheet, because in this material the grains are not aligned.

Appendix 1

The following observations provide a basis for the proposals made by the author in the present and in earlier publications concerned with the plastic deformation of cold-worked and textured polycrystalline metals.

As early as 1915, Rosenhain [7] showed extended slip-lines on iron sheet samples that had been heavily deformed after being polished. The "lines" either extended smoothly across the grain boundaries, or sets of "lines" in adjacent grains were at right angles.

Adcock [8], a few years later, revealed extended slip in cold-rolled cupro-nickel samples, the lines of slip again implying crystallographic grain alignments, bringing slip-planes parallel to what were evidently principal shear surfaces. Adcock's method was to section, metallographically prepare, and electrolytically etch the samples after partial recrystallisation, following the cold-rolling operation. Adcock claimed that during recrystallisation the new grains first developed along the lines of extended slip, thus rendering the latter visible upon etching.

Brown [9], in 1972, described the lines of extended slip that he had found on aluminium alloy samples subjected to cold-rolling; the "lines" ran parallel again to the surfaces of principal shear associated with the cold-rolling operation. Brown's method of rendering these features visible was to clad his sample in polythene before cold-rolling; the impressions of the features under discussion were observed on the polythene after its removal from the samples subsequent to cold-rolling.

French and Weinrich [10] also succeeded in revealing features similar to these in heavily deformed tensile test samples of several metals and alloys. Their method was to illuminate the prepared and etched cross-sections through their samples, using polarised light.

In every case of which the author is aware, and those cited are the outstanding examples, the deformation has been applied slowly and some special technique has been required to render the "lines" that we are discussing visible. This is the case because the "lines" exist in an already heavily cold-worked microstructure, and ordinary etching lacks the sensitivity to differentiate the lines from the matrix. The very recent method of revealing these features described by Engler *et al.* [11], well illustrates

this point. Engler's method depends on the precipitation of fine particles along the slip-lines in a cold-rolled aluminium alloy, when the samples are briefly annealed after deformation; an annealing time of 2.5 s is quoted. One may, moreover, perceive new grains nucleating along these lines on the micrograph that Engler presents, and this is, of course, the mechanism that Adcock claimed to be responsible for revealing his extended lines of slip [8].

REFERENCES

1. P.G. HODGE, *A picewise linear theory of plasticity for an initially isotropic material in plane stress*, Int. J. Mech. Sci., **22**, 21–32, 1980.
2. R. HILL, *Theoretical plasticity of textured aggregates*, Math. Proc. Camb. Phil. Soc., **85**, 179–191, 1979.
3. G. SOCHA and W. SZCZEPIŃSKI, *On experimental determination of the coefficients of plastic anisotropy in sheet metals*, Arch. Mech., **46**, 1/2, 177–190, 1994.
4. R.L. BISH, *Plane-stress deformation of a flat plate by slip between elastic elements*, Arch. Mech.,**46**, 3-12, 1994.
5. B. SPAIN, *Vector analysis*, D. Van Nostrand, 1965.
6. W. PRAGER, *Recent developments in the mathematical theory of plasticity*, J. Appl. Phys., **20**, 3, 235–241, 1949.
7. W. ROSENHAIN, *Introduction to physical metallurgy*, Constable and Co. Ltd., 1915.
8. F. ADCOCK, *The internal mechanism of cold-work and recrystallization in cupro-nickel*, J. Inst. Metals, **27**, 73–92, 1922.
9. K. BROWN, *Role of deformation and shear banding in the stability of the rolling textures of aluminium and an Al-0.8% Mg alloy*, J. Inst. Met., **100**, 341–345, 1972.
10. I.F. FRENCH and P.F. WEINRICH, *The tensile fracture mechanisms of fcc metals and alloys – a review of the influence of presssure*, J. Aust. Inst. Metals, **22**, 1, 40–50, 1977.
11. O. ENGLER, J. HIRSCH and K. LÜCKE, *Texture development in Al-1.8wt% Cu depending on the precipitation state. II. Recrystallization textures*, Acta Metall. Mater., **43**, 1, 121–138, 1995.

AERONAUTICAL AND MARITIME RESEARCH LABORATORY,
MELBOURNE, AUSTRALIA.

Received June 8, 1995.